IEEE Access
Multidisciplinary | Rapid Review | Open Access Journal

Received May 29, 2019, accepted June 11, 2019, date of publication June 19, 2019, date of current version July 8, 2019.

Digital Object Identifier 10.1109/ACCESS.2019.2923771

Multi-Source Localization Using Time of Arrival Self-Clustering Method in Wireless Sensor Networks

XINWEI GUO[1,2], ZHIFEI CHEN[1], XIAOQING HU[1], AND XIAODONG LI[1]
[1]Institute of Acoustics, Chinese Academy of Sciences, Beijing 100190, China
[2]School of Physical Sciences, University of Chinese Academy of Sciences, Beijing 100049, China

Corresponding author: Xiaoqing Hu (auxqhu@gmail.com)

This work was supported by the National Natural Science Foundation of China under Grant (11774379,61501448). The National Key Research and Development Plan (No. 2016YFC0802103), and Youth Innovation Promotion Association.

ABSTRACT The localization of multiple signal sources based on Time Of Arrival (TOA) measurements in wireless sensor networks is investigated in this paper. When the signal sources cannot be distinguished by their signatures or other unique characteristics, the correspondence between the sources and the TOA measurements at different sensors is unknown, which makes the multi-source localization problem quite challenging. A self-clustering measurement combination method is proposed for the problem. The source location estimate obtained by the hyperbolic localization algorithm is used as the clustering pattern, and the scatter of the patterns of different subsets of TOA measurements is defined as a criterion function, which is extremized by the combination of TOA measurements from the same source. A three-step heuristic clustering algorithm is pursued to resolve the TOA ambiguity, and its mean square error performance and computational complexity are also analyzed. The simulation and experiment indicate that the presented method has higher location accuracy and lower complexity compared with the existing methods.

INDEX TERMS Clustering pattern, multi-source localization, time of arrival measurement, wireless sensor networks.

I. INTRODUCTION

Wireless Sensor Networks (WSNs) consist of a number of nodes equipped with one or multiple spatially distributed sensors [1], [2]. Compared to the traditional and single sensor array comprising any number of sensors operating in tandem [3], WSNs are not limited in physical size and processing power for portable devices. WSNs also provide better spatial coverage of area of interest, which increases the probability to have a subset of sensors close to a source, yielding higher quality recordings [4]. A common issue in WSNs is the source localization, which is inherent to many applications, such as target tracking, surveillance, video conferences, robotics, and survivor localization in emergency rescue operations [5]–[9].

The source localization is to estimate the location of the source by sensing the signal emitted from the source. The methods are mainly based on three types of physical measurements: the Received Signal Strength (RSS) or energy [10]–[13], Direction Of Arrival (DOA) [14]–[17], and TOA or Time Difference Of Arrival (TDOA) [18]–[26]. In the RSS-based methods, a signal model that the energy of an acoustical signal emitted omni-directionally from a point source and propagating through ground surfaces decays at inverse of distance square is used. The model is easily influenced by the channel fading and the background noise so that the methods always fail to provide satisfactory location accuracy [27], [28]. The DOA-based localization methods estimate the source location using a set of DOA generated by the sensor array located at each node. The array requires precision mechanical tolerances relative to the reference sensor, which is very difficult during installations, and increases equipment cost and processing power. Due to the spatial resolution constraints, the location accuracy decreases as the distance between the source and node increases. In contrast, each node in the TDOA-based methods only needs one sensor to receive the source signal, and the equipment cost and the installation complexity are lower. The location accuracy is also not directly related to the baseline distance between sensors [29]. Considering these advantages of TDOA, the TDOA-based localization methods are discussed in this paper.

The associate editor coordinating the review of this manuscript and approving it for publication was Chien-Fu Cheng.

This work is licensed under a Creative Commons Attribution 3.0 License. For more information, see http://creativecommons.org/licenses/by/3.0/

These existing TDOA-based methods mainly focus on the single source localization, or assume that the signals from different sources are separable in time, frequency or both for multi-source localization [23]–[26]. However, it is very necessary to localize multiple sources simultaneously in unfriendly environments where the sensors do not have prior knowledge of individual signal feature, or the low cost sources are not equipped with unique signatures in their transmitting signals. The correspondence between the received signals at each sensor and the sources will be disorder such that the localization problem becomes more complicated. In other words, the difficulty lies in how to select one TOA measurement from each sensor to form a combination of TOA measurements corresponding to the same source for localization. There exist some methods for the multi-source localization problem. In [30], a count function given by the number of sensors agreeing on a source occurring at a space-time grid point is constructed, and estimates the source locations as the space-time grid points where the count exceeds a threshold. The method incurs high computational complexity. Furthermore, it does not directly deal with the association problem and the resulting location estimates are not accurate. In [31], a parallelized and hierarchical approach is used to solve the TOA association problem. First, for a hypothesized source emission time (obtained by discretizing the potential emission time) and an observed TOA, the source must lie on a circle with a radius equal to the propagation distance. Intersections of circles at different pairs of sensors generate candidate sources, and many of which are ''ghost'' (intersections corresponding to TOA measurements from different sources). Then, the Bayesian process and linear programming are used to refine these candidate sources. It is obvious that the location accuracy is easily influenced by the estimated propagation distance, and the computational complexity is huge due to the large number of the hypothesized emission times. In [32], the multi-source localization problem is addressed using the TOA-based convex technique (CVX-TOA). The TOA measurements at each sensor are arranged in increasing order to form a vector and then a permutation matrix representing the source-measurement association is applied to the vector, resulting in a permuted version of TOA vector. The TOA measurements with the same index in each vector corresponds to the same source, and the problem is simplified by the convex relaxation and approximation. The method requires multiple iterations to approximate the real location. The computational cost is high and the location accuracy is low. The method also estimates the source emission time, which always needs more sensors to provide information. In [33], a Portable Impact Localization System based on arrival Time Structure Analysis (TSA-PILS) is developed to localize multiple impact sources, where a search grid was constructed overlying the monitoring area and a ray model are used to obtain the model travel times. The minimum value of the errors between the real arrival times and the model travel times resulted in an unambiguous location of the source. This value is calculated by picking one sensor as the reference and then summing the timing errors of the remaining sensors relative to the reference. The method incurs complexity increasing with the size of the monitoring area, and the location accuracy heavily depends on the grid size. In fact, the underlying patterns of the TOA measurements from the same source can assemble in a cluster, and these existing methods scarcely exploit the correlation of the measurements provided by all sensors.

In this paper, a Self-Clustering Measurement Combination (SC-MC) method is proposed for the multi-source localization problem. The source location estimate acquired by the hyperbolic localization algorithm is used as the clustering patterns, and the volume of the scattered patterns of different subsets of TOA measurements is defined as a criterion function to measure the clustering quality of a combination of TOA measurements from different sensors. The SC-MC is formulated as an optimal problem, and a three-step heuristic clustering algorithm is presented to resolve the TOA ambiguity. The method does not require a grid search, and has higher location accuracy and lower computational cost.

The remainder of the paper is organized as follows. In Section II, the signal model is introduced. In Section III, the SC-MC problem is formulated and a three-step heuristic clustering algorithm for multi-source localization is presented. The performance of the algorithm is analyzed in Section IV. In Section V, simulation and experiment results are shown. Section VI concludes this paper. For the ease of reading, some proofs are included in the Appendix.

II. SIGNAL MODEL

Consider M distributed sensors deployed at known locations denoted by the column vectors $\mathbf{s}_i \in \mathbb{R}^2, i \in [1, M]$ within a two-dimensional region that we wish to monitor. These sensors are synchronized by the Pulse Per Second (PPS) of Global Position System (GPS). The problem is to localize N sources whose locations are denoted by the vectors $\boldsymbol{u}_j \in \mathbb{R}^2, j \in [1, N]$, as shown in Fig. 1(a).

Note that we focus on a propagation environment in which either a line-of-sight (LOS) path exists or scatterers are near the sources or the sensors to provide a near LOS path. Accordingly, the lth, $l \in [1, N]$ TOA measurement $t_{i,l}^j$ generated by the jth source at the ith sensor can be expressed by

$$t_{i,l}^j = ||\boldsymbol{u}_j - \mathbf{s}_i||/c + t_j + \gamma_{i,l}^j, \tag{1}$$

where c is the signal propagation speed (acoustic sensors are used in this paper and $c = 340$ m/s unless stated otherwise), $||\cdot||$ denotes the two-norm of a vector, and t_j is the time where the jth source signal starts to be emitted from $\boldsymbol{u}_j$. $\gamma_{i,l}^j$ is the TOA measurement noise, and these noises are assumed to be mutually independent and identically distributed zero-mean Gaussian variables with the standard deviation σ.

There exists one important problem that the correspondence between the sources and the TOA measurements at different sensors are unknown during the localization process. When different sources are not equipped with distinct signatures for identifying themselves or the sensors are not

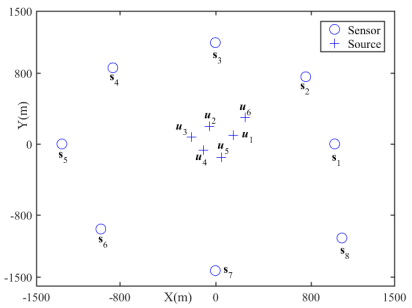

(a)

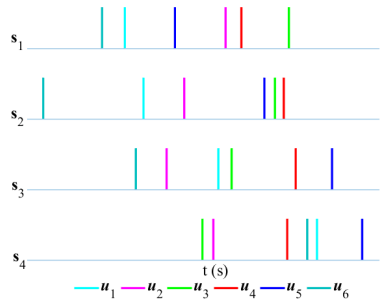

(b)

FIGURE 1. (a) A monitoring area with $M = 8$ sensors and $N = 6$ sources. (b) The order of TOA measurements at different sensors (the bars with the same color mean that these TOA measurements correspond to the same source).

able to detect such signatures due to lack of prior information, the sensors can only sense the arriving signals without knowing from which sources these signals originate [32], as shown in Fig. 1(b). The simple strategy that associates the jth TOA measurement at each sensor to localize the source will fail. To capture the challenging problem, the paper proposes a SC-MC method.

III. MULTI-SOURCE LOCALIZATION

A. HYPERBOLIC LOCALIZATION ALGORITHM

We firstly review the hyperbolic localization algorithm [18]. For the combination $\{t^j_{1,l}, \cdots, t^j_{i,l}, \cdots, t^j_{M,l}\}$ of TOA measurements from the same source $\boldsymbol{u}_j$, the location estimate $\hat{\boldsymbol{u}}_j$ can be directly obtained by the hyperbolic localization algorithm. Let $r_{j,i} = ||\boldsymbol{u}_j - \mathbf{s}_i||$ be the distance between the jth source and the ith sensor, and the TDOA $\Delta t_{j,i,1} = t^j_{i,l} - t^j_{1,l}$ with respect to the TOA measurement of the reference sensor (say $\mathbf{s}_1$), is used to obtain the range difference of arrival

$$r_{j,i,1} = c * \Delta t_{j,i,1} = r_{j,i} - r_{j,1}, \quad i = 2, 3, \cdots, M. \tag{2}$$

Let $\boldsymbol{\varphi}_j = [\boldsymbol{u}_j^T, r_{j,1}]^T$ be an unknown column vector, and takes the squares of (2) to obtain the following equation

$$r^2_{j,i,1} - \mathbf{s}_i^T\mathbf{s}_i + \mathbf{s}_1^T\mathbf{s}_1 = -2[(\mathbf{s}_i - \mathbf{s}_1)^T, r_{j,i,1}]\boldsymbol{\varphi}_j. \tag{3}$$

Then, the weighted least square estimation $\hat{\boldsymbol{\varphi}}_j$ of $\boldsymbol{\varphi}_j$ can be obtained as

$$\begin{aligned}\hat{\boldsymbol{\varphi}}_j &= \arg\ \min\ \{(\mathbf{h}_j - \Gamma_j\boldsymbol{\varphi}_j)^T\Psi_j^{-1}(\mathbf{h}_j - \Gamma_j\boldsymbol{\varphi}_j)\} \\ &= (\Gamma_j^T\Psi_j^{-1}\Gamma_j)^{-1}\Gamma_j^T\Psi_j^{-1}\mathbf{h}_j, \quad \Psi_j = c^2\mathbf{B}_j\mathbf{Q}\mathbf{B}_j, \end{aligned} \tag{4}$$

where

$$\begin{aligned}\mathbf{h}_j &= \frac{1}{2}\begin{bmatrix} r^2_{j,2,1} - \mathbf{s}_2^T\mathbf{s}_2 + \mathbf{s}_1^T\mathbf{s}_1 \\ r^2_{j,3,1} - \mathbf{s}_3^T\mathbf{s}_3 + \mathbf{s}_1^T\mathbf{s}_1 \\ \vdots \\ r^2_{j,M,1} - \mathbf{s}_M^T\mathbf{s}_M + \mathbf{s}_1^T\mathbf{s}_1 \end{bmatrix}, \\ \Gamma_j &= -\begin{bmatrix} (\mathbf{s}_2 - \mathbf{s}_1)^T & r_{j,2,1} \\ (\mathbf{s}_3 - \mathbf{s}_1)^T & r_{j,3,1} \\ \vdots & \vdots \\ (\mathbf{s}_M - \mathbf{s}_1)^T & r_{j,M,1} \end{bmatrix}, \\ \mathbf{B}_j &= \mathrm{diag}\{r_{j,2}, \cdots, r_{j,4}, \cdots, r_{j,M}\}. \end{aligned} \tag{5}$$

In (4), $\mathbf{Q}$ is the covariance matrix of the TDOA vector $[\Delta t_{j,2,1}, \cdots, \Delta t_{j,i,1}, \cdots, \Delta t_{j,M,1}]^T$ with diagonal elements of 2 and other elements of 1, and $\mathbf{B}_j$ is the diagonal matrix formed by the elements $r_{j,i}$. Since $\mathbf{B}_j$ contains the true source location $\boldsymbol{u}_j$ and is unknown, it is firstly approximated through an initial estimate of $\boldsymbol{\varphi}_j$, say $\hat{\boldsymbol{\varphi}}_{j,1}$, When setting $\mathbf{B}_j$ to identity matrix. Then, the diagonal element $r_{j,i}$ is approximated by $||\hat{\boldsymbol{\varphi}}_{j,1}(1:2) - \mathbf{s}_i||$ ($\hat{\boldsymbol{\varphi}}_{j,1}(1:2)$ denotes a subvector formed by the first two elements of $\hat{\boldsymbol{\varphi}}_{j,1}$). Finally, the location estimate $\hat{\boldsymbol{u}}_j = \hat{\boldsymbol{\varphi}}_j(1:2)$ is obtained by (4). More details can be found in [18].

B. SELF-CLUSTERING MEASUREMENT COMBINATION

The Self-Clustering Measurement Combination (SC-MC) method effectively aggregates the location estimate patterns of the associated TOA measurements to find the combination of TOA measurements from the same source.

The location estimate $\hat{\boldsymbol{u}}_j$ approximately obeys a normal distribution with mean vector $\boldsymbol{u}_j$ and positive-define covariance matrix $\boldsymbol{\Sigma}_j = \mathbb{E}[(\hat{\boldsymbol{u}}_j - \boldsymbol{u}_j)(\hat{\boldsymbol{u}}_j - \boldsymbol{u}_j)^T]$. The sample points drawn from the normal distribution tend to fall in a cluster, whose center and shape are determined by the mean vector and the covariance matrix, respectively. The squared Mahalanobis Distance (MD) [34] between the sample points and the cluster center $\boldsymbol{u}_j$ is given as

$$\beta_j^2 = (\hat{\boldsymbol{u}}_j - \boldsymbol{u}_j)^T(\boldsymbol{\Sigma}_j)^{-1}(\hat{\boldsymbol{u}}_j - \boldsymbol{u}_j). \tag{6}$$

The loci of the sample points of constant density are ellipsoids for which the β_j is constant. The volume of ellipsoids measures the scatter of the sample points about mean and is given by

$$V_j = v_2|\boldsymbol{\Sigma}_j|^{1/2}\beta_j^2, \tag{7}$$

where v_2 is the volume of a two-dimensional unit sphere. Thus, the determinant $|\boldsymbol{\Sigma}_j|^{1/2}$ of the covariance matrix is used as a criterion function to measure the scatter of the sample points ($|\boldsymbol{\Sigma}_j|^{1/2}$ and V_j are interchangeable throughout

the paper because they are mathematically equivalent) [34]. A larger $|\boldsymbol{\Sigma}_j|^{1/2}$ means that the sample points are more scattered.

For a combination of TOA measurements from two or more sources, e.g., $\{t^j_{1,l}, \cdots, t^j_{i-1,l}, t^{\lambda}_{i,l}, t^j_{i+1,l}, \cdots, t^j_{M,l}\}$, $\lambda \in [1, N]$ and $\lambda \neq j$, in order to distinguish from the previous variables, $\hat{\boldsymbol{\varphi}}_j$, $\hat{\boldsymbol{u}}_j$, $r_{j,i,1}$, Γ_j, $\mathbf{h}_j$, Ψ_j are replaced by $\hat{\boldsymbol{\varphi}}^e_j$, $\hat{\boldsymbol{u}}^e_j$, $r^e_{j,i,1}$, Γ^e_j, $\mathbf{h}^e_j$, Ψ^e_j. From (4), the ghost target location estimate $\hat{\boldsymbol{u}}^e_j = \hat{\boldsymbol{\varphi}}^e_j(1:2)$ is obtained based on the equation

$$\hat{\boldsymbol{\varphi}}^e_j = (\Gamma^{eT}_j \Psi^{e^{-1}}_j \Gamma^e_j)^{-1} \Gamma^{eT}_j \Psi^{e^{-1}}_j \mathbf{h}^e_j. \tag{8}$$

In the above equation, the mean and the covariance matrix of $\hat{\boldsymbol{u}}^e_j$ are assumed to be $\mathbb{E}\{\hat{\boldsymbol{u}}^e_j\} = \boldsymbol{u}^e_j$ and $\boldsymbol{\Sigma}^e_j = \mathbb{E}\{(\boldsymbol{u}^e_j - \hat{\boldsymbol{u}}^e_j)(\boldsymbol{u}^e_j - \hat{\boldsymbol{u}}^e_j)^T\}$, respectively.

In fact, the actual source location estimate is $\hat{\boldsymbol{u}}_j = \hat{\boldsymbol{\varphi}}_j(1:2)$, where $\hat{\boldsymbol{\varphi}}_j(1:2)$ is calculated as

$$\begin{aligned}\hat{\boldsymbol{\varphi}}_j = ((\Gamma^e_j + \Delta\Gamma_j)^T \Psi^{e^{-1}}_j (\Gamma^e_j + \Delta\Gamma_j))^{-1} \\ \times (\Gamma^e_j + \Delta\Gamma_j)^T \Psi^{e^{-1}}_j (\mathbf{h}^e_j + \Delta\mathbf{h}_j).\end{aligned} \tag{9}$$

The derivation can be found in Appendix A. The ghost target location estimate $\hat{\boldsymbol{u}}^e_j$ has a deviation compared with $\hat{\boldsymbol{u}}_j$ and is not optimum. From Appendix B, the determinant $|\boldsymbol{\Sigma}^e_j|$ is larger than $|\boldsymbol{\Sigma}_j|$, which points out that the sample points drawn from the normal distribution with mean vector $\boldsymbol{u}^e_j$ and covariance matrix $\boldsymbol{\Sigma}^e_j$ are more scattered than those drawn from the normal distribution with mean vector $\boldsymbol{u}_j$ and covariance matrix $\boldsymbol{\Sigma}_j$.

For a given combination of TOA measurements, if the TOA measurements stem from the same source, e.g., $\{t^j_{1,l}, \cdots, t^j_{i,l}, \cdots, t^j_{M,l}\}$, the location estimates corresponding to its subsets of TOA measurements, e.g., $\{t^j_{1,l}, \cdots, t^j_{i,l}, \cdots, t^j_{M-2,l}\}$, are clustered around the true source location $\boldsymbol{u}_j$. Otherwise, the location estimates corresponding to different subsets of TOA measurements will deviate from $\boldsymbol{u}_j$ and are more scattered, as shown in Fig. 2. It is obvious that the volume of the ellipsoids corresponding to the false combinations of TOA measurements becomes larger.

For ease of analysis, it assumes that the l_ith, $l_i \in [1, N]$ TOA measurement $t^{j_i}_{i,l_i}$ at the ith sensor corresponds to the $j^{l_i}_i$th, $j^{l_i}_i \in [1, N]$ source. In particular, $j^{l_1}_1 = l_1$ (the jth TOA measurement at the 1st sensor corresponds to the jth source). For the candidate combination $C_{j,p} = \{t^j_{1,j}, \cdots, t^{j_i}_{i,l_i}, \cdots, t^{j_M}_{M,l_M}\}, p \in [1, N^{M-1}]$ of the jth source, $\hat{\boldsymbol{u}}_{j,p,d} \in \mathbb{R}^2, d \in [1, D]$ are assumed to be the location estimates corresponding to its D subsets of TOA measurements, and the ellipsoid volume $V_{j,p}$ is approximated by

$$\begin{aligned}V_{j,p} &\approx \left| \frac{1}{D} \sum_{d=1}^{D} (\hat{\boldsymbol{u}}_{j,p,d} - \bar{\boldsymbol{u}}_{j,p})(\hat{\boldsymbol{u}}_{j,p,d} - \bar{\boldsymbol{u}}_{j,p})^T \right|^{1/2}, \\ \bar{\boldsymbol{u}}_{j,p} &= \frac{1}{D} \sum_{d=1}^{D} \hat{\boldsymbol{u}}_{j,p,d}.\end{aligned} \tag{10}$$

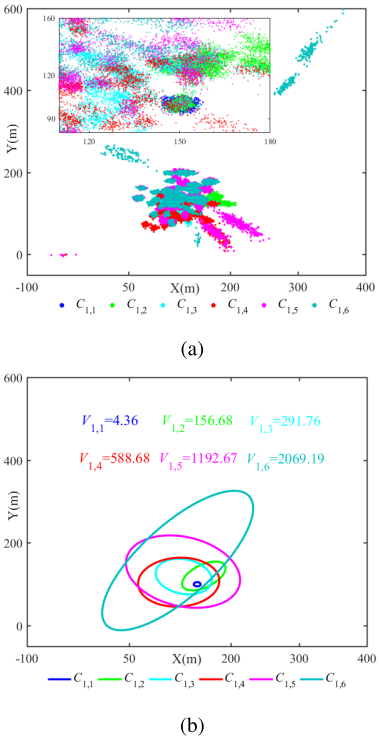

FIGURE 2. The scatter of the location estimates corresponding to subsets of different combinations of TOA measurements. $C_{1,p}, p \in [1, 6]$ are the candidate combinations of TOA measurements for the 1st source in Fig. 1, where there are $(p-1)$ TOA measurements from other sources, and $V_{1,p}$ is the volume of ellipsoid. (a)The colored dots represent the location estimates corresponding to subsets of different combinations and are obtained through 100 Monte-Carlo runs under $\sigma = 0.01$ scenario. (b) The colored ellipses represent the error ellipses of the location estimates of different combinations with a 0.9 confidence interval.

The goal is to find the optimal combination of TOA measurements that minimizes the criterion function defined by the ellipsoid volume,

$$\hat{C}_{j,p} = \arg \min_{C_{j,p}} V_{j,p}. \tag{11}$$

When the location estimate patterns are clustered, the TOA measurements containing the patterns are also clustered, and the relationship between the patterns and the TOA measurements is made explicit.

C. A THREE-STEP HEURISTIC CLUSTERING ALGORITHM

The problem to find the optimal combination of TOA measurements is known to be NP-complete [35], [36]. The Exhaustive Maximum Likelihood (EML) method calculates the volume of the ellipsoids corresponding to all possible combinations of TOA measurements. When the number of sources or sensors increases, the number of combinations will increase dramatically so that the computational complexity is unacceptable. For this reason, a more efficient, albeit suboptimal, heuristic clustering algorithm of the SC-MC is proposed (see Fig. 3). It starts by selecting the initial sensors and combining their TOA measurements, thus obtaining the potential source locations. Then, the TOA measurements of

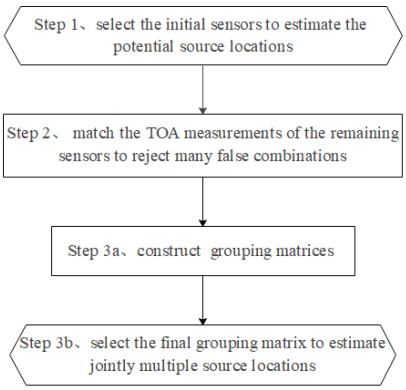

FIGURE 3. Flow chart of a three-step heuristic clustering algorithm of the SC-MC.

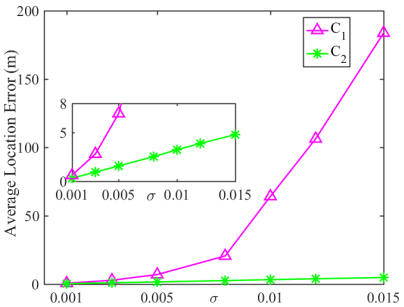

FIGURE 4. Comparison of average location errors of different initial sensors. C_1 and C_2 are two correct combinations of TOA measurements for the 1st source in Fig. 1. In C_1, s_2, s_3, s_4 and s_5 are used. In C_2, s_1, s_3, s_6, s_7 are used. The sensors in C_1 are only on one side of the monitoring area. The average location errors are obtained by 1000 Monte-Carlo runs under different noise levels.

the remaining sensors are matched with the potential source locations to reject many false combinations of TOA measurements. Finally, construct grouping matrices based on the chosen combinations of TOA measurements to estimate jointly multiple source locations.

1) SELECT THE INITIAL SENSORS TO ESTIMATE THE POTENTIAL SOURCE LOCATIONS

Since the SC-MC method finds an approximation solution to a problem with NP-complete, it might suffer from convergence to a local minimum; thus the choice of the initial sensors should provide as accurate estimates of the potential source locations as possible, which requires that the sensors should surround the monitoring area [37]. As shown in Fig. 4, the location error will be larger if the sensors are only on one side of the monitoring area.

Specifically, select $n, n \geq 4$ (the closed-form solution of the hyperbolic localization algorithm requires at least 4 sensors within a two-dimensional area [18]) sensors and combine their TOA measurements, as shown in Algorithm 1. Based on the TOA measurements with indices in each row of the matching matrix $\mathbf{E}_j$, the $N^{(n-1)}$ potential source locations $\hat{\boldsymbol{u}}_{j,k}, k \in [1, N^{(n-1)}]$ for the jth source can be obtained by the hyperbolic localization algorithm.

Algorithm 1 Combine the TOA Measurements of the n Initial Sensors

```
for j = 1 to N do
    k = 0
    E_j is an empty matrix
    for l_2 = 1 to N do
        ⋮
        for l_n = 1 to N do
            k = k + 1
            Row(E_j)_k = [j, l_2, ··· , l_n]; // the n indices
            are stored in the kth row of E_j
            Row(E_j)_k ⇒ û_{j,k}; // estimate the potential
            source locations
        end
    end
end
```

2) MATCH THE TOA MEASUREMENTS OF THE REMAINING SENSORS TO REJECT MANY FALSE COMBINATIONS

The remaining sensors are added one by one and their TOA measurements are matched with the potential locations $\hat{\boldsymbol{u}}_{j,k}, k \in [1, N^{(n-1)}]$ to reject many false combinations of TOA measurements.

From the potential source location $\hat{\boldsymbol{u}}_{j,k}$ to the sensor pair $(1, m)$, $m = n + 1$, the model propagation time difference $\mathrm{MT}_{j,k,1,m}$ is given by

$$\mathrm{MT}_{j,k,1,m} = (||\hat{\boldsymbol{u}}_{j,k} - \mathbf{s}_m|| - ||\hat{\boldsymbol{u}}_{j,k} - \mathbf{s}_1||)/c. \quad (12)$$

The TDOA error $\mathrm{TE}_{j,k,1,m}$ is defined by

$$\mathrm{TE}_{j,k,1,m} = \mathrm{MT}_{j,k,1,m} - (t^{\hat{l}_m}_{m,\hat{l}_m} - t^{j}_{1,j}),$$
$$\hat{l}_m = \arg \min_{l_m \in [1,N]} \mathrm{MT}_{j,k,1,m} - (t^{l_m}_{m,l_m} - t^{j}_{1,j}). \quad (13)$$

The basic idea of this step is that if the TOA measurements in a combination are from the same source, the corresponding hyperbolas will intersect at the same location $\boldsymbol{u}_j$ in a noise-free environment. Since the TOA measurements are corrupted by noises, the credibility of the combination$\{t^{j}_{1,j}, \cdots, t^{j_4}_{4,l_4}, \cdots, t^{\hat{l}_m}_{m,\hat{l}_m}\}$ from the same source is represented by $\mathrm{TE}_{j,k,1,m}$, where a smaller $\mathrm{TE}_{j,k,1,m}$ implies a higher credibility. Therefore, a total number of N^{n-1} errors $\mathrm{TE}_{j,k,1,m}$ are sorted in ascending order and the indices $\{j, \cdots, 4, \cdots, \hat{l}_m\}$ of the top ρ combinations are recorded in the matching matrix $\mathbf{E}_j$, which is a ρ-by-m matrix. In order to avoid missing the true combination, ρ is generally assigned to a large value, e.g., $\rho = N^{(n-1)}/2$.

The process is repeated for $m \in [n + 2, M]$, where the TDOA error $\mathrm{TE}_{j,k,1,m}$ and ρ are updated. The step is performed for $j \in [1, N]$ and the number of false combinations is greatly reduced. More details can be found in Algorithm 2.

Algorithm 2 Match the TOA Measurements of the Remaining Sensors

for $j = 1$ *to* N **do**
  $\rho = N^{(n-1)}/2$;
  for $m = n+2$ *to* M **do**
    for $k = 1$ *to* ρ **do**
      //calculate TDOA error
      $\mathrm{TE}_{j,k,1,m} =$
      $\mathrm{MT}_{j,k,1,m} - (t^{\hat{j}_m^m}_{m,\hat{l}_m} - t^{j}_{1,j}) + \mathrm{TE}_{j,k,1,m-1}$;
      $\mathrm{Row}(\mathbf{E}_j)_k = [\mathrm{Row}(\mathbf{E}_j)_k, \hat{l}_m]$; // associate the index of TOA measurement
    end
    $[\mathrm{Val},\mathrm{Ind}] = \mathrm{sort}(\mathrm{TE}_{j,1:\,\rho,1,m})$; //$\rho$ errors $\mathrm{TE}_{j,1:\,\rho,1,m}$ are sorted in ascending order; Val is the error set and Ind is the index set
    $\rho = \rho/2$; // each time takes half the number of combinations previously taken
    $\mathbf{U}$ is an empty matrix;
    for $k = 1$ *to* ρ **do**
      $\mathrm{TE}_{j,k,1,m} = \mathrm{Val}(k)$; //update TDOA error
      $\mathrm{Row}(\mathbf{U})_k = \mathrm{Row}(\mathbf{E}_j)_{\mathrm{Ind}(k)}$; //the Ind($k$)th row of $\mathbf{E}_j$ is assigned to the kth row of $\mathbf{U}$
    end
    $\mathbf{E}_j = \mathbf{U}$; // update the matching matrix
  end
end

Algorithm 3 Construct Grouping Matrices of the N Sources

$q = 0$
for $q_1 = 1$ *to* ρ_2 **do**
  for $q_2 = 1$ *to* ρ_2 **do**
    ⋮
    for $q_N = 1$ *to* ρ_2 **do**
      $\mathbf{F} = \begin{bmatrix} Row(\mathbf{E}_1)_{q_1} \\ Row(\mathbf{E}_2)_{q_2} \\ \vdots \\ Row(\mathbf{E}_N)_{q_N} \end{bmatrix}$; // construct one N-by-M grouping matrix
      if $\mathbf{F}$ *does not have duplicated index in each column* **then**
        $q = q + 1$;
        $\mathbf{G}_q = \mathbf{F}$;
      else
        assuming that the ith column has duplicated indices x
        if *the ith sensor has one TOA measurement* t *satisfying* $|t - t^{j_i^x}_{i,x}| < \tau$ **then**
          $q = q + 1$;
          $\mathbf{G}_q = \mathbf{F}$;
        end
      end
    end
  end
end

3) CONSTRUCT GROUPING MATRICES TO ESTIMATE JOINTLY MULTIPLE SOURCE LOCATIONS

After the above matching step, there are ρ chosen combinations of TOA measurements for each source. From (10), the volume of ellipsoid corresponding to each combination in the matching matrix $\mathbf{E}_j, j \in [1, N]$ is easily obtained. For each source, ρ volume of ellipsoids is sorted in ascending order and the top ρ_2 (ρ_2 and the following ρ_3 are usually assigned to some large values to avoid missing the true combinations, e.g., $\rho_2 = N$, and $\rho_3 = 2N$) related combinations are kept in $\mathbf{E}_j$.

By considering the N matching matrices $\mathbf{E}_j$ where each matrix contributes ρ_2 combinations, there are $(\rho_2)^N$ different possibilities to construct one N-by-M grouping matrix, whose jth row corresponds to the jth source. In general, each TOA measurement can be used for only one source and the grouping matrix with duplicated indices in a column would be deleted. However, if one sensor has two very close TOA measurements whose interval is less than τ (discussed in V-B), they can be replaced by each other, which does not lead to significantly larger location error and the grouping matrix should also be accepted. More details can be found in Algorithm 3. The number of the grouping matrices is much less than $(\rho_2)^N$. Let V_q^g be the sum of the volume of ellipsoids corresponding to the N combinations in matrix $\mathbf{G}_q$. The final selected grouping matrix $\hat{\mathbf{G}}_q$ is as follows

$$\hat{\mathbf{G}}_q = \arg \min_{\mathbf{G}_q} V_q^g. \tag{14}$$

Based on the TOA measurements with indices in each row of $\hat{\mathbf{G}}_q$, the location estimates of the N sources can be obtained by the hyperbolic localization algorithm.

To further reduce the computational cost, the N sources can be subdivided into two cells, e.g., $\{\boldsymbol{u}_1, \boldsymbol{u}_2, \cdots, \boldsymbol{u}_{[N/2]}\}$, $\{\boldsymbol{u}_{[N/2]+1}, \boldsymbol{u}_{[N/2]+2}, \cdots, \boldsymbol{u}_N\}$ ($[\cdot]$ rounds the element to the nearest integer). The matching matrices in each cell are used to construct independently grouping matrices, and then the top ρ_3, e.g., $\rho_3 = 2N$ grouping matrices in each cell are selected to construct jointly the final grouping matrices.

IV. PERFORMANCE ANALYSIS OF THE SC-MC

A. CRAMER-RAO LOWER BOUND FOR MULTI-SOURCE LOCATION

Cramer-Rao Lower Bound (CRLB) that provides a lower bound on the mean square error of the location estimate is widely used to assess the performance of an estimator. In this paper, the CRLB of the location estimates

$\hat{\boldsymbol{u}} = [\hat{\boldsymbol{u}}_1^T, \cdots, \hat{\boldsymbol{u}}_N^T]^T$ is given by

$$P\sum_{j=1}^{N}\mathbb{E}\{||\hat{\boldsymbol{u}}_j - \boldsymbol{u}_j||^2\} \geq \sum_{j=1}^{N}\text{trace}(\Omega_j),$$

$$\Omega_j = c^2\sigma^2(\Phi_j^T\mathbf{Q}^{-1}\Phi_j)^{-1},\ \mathbf{e}_{j,i} = \mathbf{s}_i - \boldsymbol{u}_j,$$

$$\Phi_j = \begin{bmatrix} \frac{\mathbf{e}_{j,1}(1)}{r_{j,1}} - \frac{\mathbf{e}_{j,2}(1)}{r_{j,2}} & \frac{\mathbf{e}_{j,1}(2)}{r_{j,1}} - \frac{\mathbf{e}_{j,2}(2)}{r_{j,2}} \\ \frac{\mathbf{e}_{j,1}(1)}{r_{j,1}} - \frac{\mathbf{e}_{j,3}(1)}{r_{j,3}} & \frac{\mathbf{e}_{j,1}(2)}{r_{j,1}} - \frac{\mathbf{e}_{j,3}(2)}{r_{j,3}} \\ \vdots & \vdots \\ \frac{\mathbf{e}_{j,1}(1)}{r_{j,1}} - \frac{\mathbf{e}_{j,M}(1)}{r_{j,M}} & \frac{\mathbf{e}_{j,1}(2)}{r_{j,1}} - \frac{\mathbf{e}_{j,M}(2)}{r_{j,M}} \end{bmatrix}, \quad (15)$$

where $\mathbf{e}_{j,i}(1)$ and $\mathbf{e}_{j,i}(2)$ are the first and second elements of the vector $\mathbf{e}_{j,i}$, respectively [18].

B. COMPUTATIONAL COMPLEXITY ANALYSIS

For simplicity, each hyperbolic localization and each matching of TOA measurement is counted as one operation (in fact, the complexity of each hyperbolic localization is higher than each matching of TOA measurement). The analysis is shown in Table 1.

The number of the operations and the grouping matrices are $N^n(1 + 2N - \frac{N}{2^{M-n-1}}) + \rho DN$ and $2(\rho_2)^{\frac{N}{2}} + (\rho_3)^2$ in SC-MC, respectively. In contrast, in the EML method, the number of the operations and the grouping matrices are $N^M D$ and $N^{(M-1)N}$, respectively. The number of computations in the EML method increases exponentially and is far higher than SC-MC.

V. NUMERICAL SIMULATIONS AND EXPLOSION EXPERIMENTS

The section includes three subsections of performance comparison, parameter analysis, and explosion experiments. In V-A, the location performance of the SC-MC is compared with the Genie-Aided method (GA) [32], EML, TSA-PILS and CVX-TOA. In V-B, the relationship between the location accuracy of the SC-MC method and some parameters is discussed. In V-C, the explosion experiments were carried out to verify the SC-MC method.

A. PERFORMANCE COMPARISON

The location performance of the SC-MC is compared with the GA, EML, TSA-PILS and CVX-TOA by their computational efficiency and location accuracy. The GA method with ideal source-measurement associations is used as a reference relative to other methods [32]. The details about CVX-TOA and TSA-PILS can be found in Section I. TSA-PILS is a direct approach that finds the source location by searching all possible positions and selecting the one that best explains the TOA measurements. SC-MC and CVX-TOA are the indirect approaches that estimate the location of the source

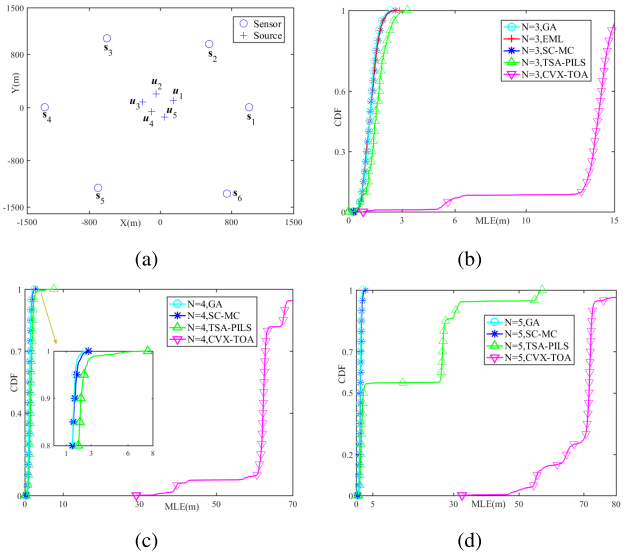

FIGURE 5. Comparison of the location accuracy of different methods under $\sigma = 0.005$ condition. (a) the locations of the sensors and the sources; (b) the CDF of MLE for the first 3 sources; (c) the CDF of MLE for the first 4 sources; (d) the CDF of MLE for the 5 sources.

based on the positioning parameters such as TOA or TDOA. In CVX-TOA, the occurrence time of each source also needs to be estimated, which is not required in SC-MC. The location accuracy is characterized by the Cumulative Distribution Function (CDF) of the Multi-source Location Error (MLE), which is computed as

$$\text{MLE} = \frac{1}{N}\sum_{j=1}^{N}||\boldsymbol{u}_j - \hat{\boldsymbol{u}}_j||. \quad (16)$$

The CDF of the MLE is given by

$$f_{\text{MLE}}(\kappa) = Pr(\text{MLE} \leq \kappa), \quad (17)$$

where the right-hand side represents the probability that the MLE takes a value less than or equal to κ.

In this simulation, $M = 6$ sensors are deployed in a monitoring area of approximately 2500 meters by 2500 meters. $N = 5$ sources are located at $\boldsymbol{u}_1 = [150, 100]^T, \boldsymbol{u}_2 = [-50, 200]^T, \boldsymbol{u}_3 = [-200, 80]^T, \boldsymbol{u}_4 = [-100, -70]^T$, and $\boldsymbol{u}_5 = [50, -150]^T$, as shown in Fig. 5(a). Three scenarios with different number of the sources are considered, where the first 3 sources, the first 4 sources and all 5 sources are used separately.

For each scenario, 1000 Monte-Carlo runs are performed to obtain the CDF of MLE (the computational cost of EML is huge and its CDF curves are not shown for $N = 4$ sources and $N = 5$ sources), and the results are shown in Fig. 5(b), (c), and (d). It is quite clear that the SC-MC, EML, and GA have almost the same CDF curve, which indicates that SC-MC and EML can find the correct combinations of TOA measurements. The location error of TSA-PILS is similar to GA and SC-MC in the case of fewer sources ($N = 3$), but becomes higher when the number of the sources

TABLE 1. The number of computations for SC-MC and EML.

	SC-MC			EML
	Step1	Step2	Step3	Step3
hyperbolic localization	N^n	0	ρDN	$N^M D$
matching of TOA measurements	0	$N^{n+1}(2-\frac{1}{2^{M-n-1}})$	0	0
grouping matrix	0	0	$2(\rho_2)^{N/2}+(\rho_3)^2$	$N^{(M-1)N}$

[1] EML does not have Step 1 or Step 2.

TABLE 2. Comparison of the estimation bias of different methods (m).

σ	0.005	0.01	0.015	0.02
SC-MC	0.056	0.324	0.687	1.059
TSA-PILS	0.067	0.489	2.990	8.494
CVX-TOA	13.092	13.459	14.133	16.584

[1] The $M = 6$ sensors and the first 3 sources $\boldsymbol{u}_1, \boldsymbol{u}_2$, and $\boldsymbol{u}_3$ in Fig. 5(a) are used.

TABLE 3. CRLB versus AMSE of SC-MC, TSA-PILS, and CVX-TOA (m^2).

σ	0.005	0.01	0.015	0.02
CRLB	1.9	7.8	17.5	31.1
SC-MC	2.0	9.4	23.7	45.5
TSA-PILS	3.5	29.8	274.0	784.1
CVX-TOA	271.4	395.3	887.0	1647.1

[1] The $M = 6$ sensors and the first 3 sources $\boldsymbol{u}_1, \boldsymbol{u}_2$, and $\boldsymbol{u}_3$ in Fig. 5(a) are used.

is more ($N = 4$ or 5). Especially, the larger location error of TSA-PILS indicates the mismatch that the ghost target location estimate corresponding to the false combination of TOA measurements is accepted eventually, often occurred in the case of more sources, such as $N = 5$. In the CVX-TOA, the location error increases sharply when the number of the sources increases and the location accuracy is the worst.

Table 2 gives the Estimation Bias (EB) of SC-MC, TSA-PILS, and CVX-TOA, where the EB is computed by

$$\text{EB} = \frac{1}{N}\sum_{j=1}^{N} ||\mathbb{E}\{\hat{\boldsymbol{u}}_j - \boldsymbol{u}_j\}||. \tag{18}$$

From Table 2, the SC-MC has the smallest estimation bias, and the estimation bias of TSA-PILS is smaller than CVX-TOA, which indicates that the SC-MC has the best consistency.

To further evaluate the location accuracy of these methods, the Average Mean Square Error (AMSE) of the location estimate is compared with the CRLB given in Section IV-A. The AMSE is defined by

$$\text{AMSE} = \frac{1}{N}\sum_{j=1}^{N} \mathbb{E}\{||\boldsymbol{u}_j - \hat{\boldsymbol{u}}_j||^2\}. \tag{19}$$

Table 3 lists the AMSE results. It can be observed that the AMSE of TSA-PILS and CVX-TOA increase dramatically as the noise level σ increases and are far higher than CRLB. The AMSE of SC-MC is closer to CRLB and can even attain the CRLB when the noise level σ is lower. The above results show that SC-MC has very excellent location accuracy in the case of high noise level and dense sources.

TABLE 4. Comparison of the computation time of different methods (s).

	GA	SC-MC	TSA-PILS	CVX-TOA	EML
N=3	0.0006	0.065	1.445	7.599	54.413
N=4	0.0007	0.128	3.147	10.221	—[2]
N=5	0.0009	0.305	7.035	13.228	—

[1] The three scenarios used here are shown in Fig. 5, and the computation time is an average of 1000 run times.
[2] The computation time is far higher than 10000 s. For convenience, it is not shown here.

Based on the above three scenarios, a comparison of the computation times of different methods is shown in Table 4. These simulations are performed on an Intel(R) Core(TM) i5-7300HQ computer with 2.5GHz CPU and 8GB RAM using MatLab scripts. When the number N of the sources increases, the number of the combinations increases, which leads to higher computational cost for all methods. The computation cost of GA is the lowest since the hyperbolic localization algorithm is noniterative and gives an explicit solution. The EML method tries all possible combinations of TOA measurements and then select the most likely one, which leads to the highest computational cost. In contrast, SC-MC significantly reduces the computational cost compared with EML. Because a grid search step is needed in the TSA-PILS method, its computational cost is much higher than the SC-MC. In the CVX-TOA, the location estimate is obtained by a convex optimization technique, which requires multiple iterative operations, and the computation cost is higher than the GA, SC-MC, and TSA-PILS. This results show that the SC-MC is more computationally efficient than the existing methods.

B. PARAMETER ANALYSIS

This subsection mainly discusses the relationship between the location accuracy of the SC-MC method and the sensor location error, the TOA measurements interval τ (proposed in III-C.3), TOA measurement noise σ, the number N of targets, and the number M of sensors.

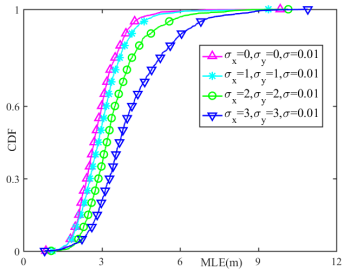

FIGURE 6. Comparison of the location accuracy under different sensor location error conditions. The $M = 6$ sensors and $N = 5$ sources in Fig. 5(a) are used.

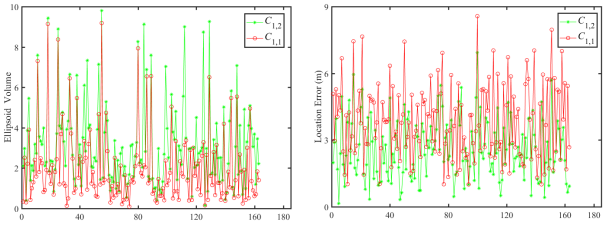

(a) (b)

FIGURE 7. Comparison of the ellipsoid volume and location error between $C_{1,1} = \{t^1_{1,1}, t^1_{2,1}, t^1_{3,3}, t^1_{4,5}, t^2_{5,4}, t^1_{6,3}\}$ and $C_{1,2} = \{t^1_{1,1}, t^1_{2,1}, t^1_{3,3}, t^1_{4,5}, t^1_{5,5}, t^1_{6,3}\}$, where the $M = 6$ sensors and $N = 5$ sources in Fig. 5(a) are used. The interval $\Delta t = |t^2_{5,4} - t^1_{5,5}| \approx 0.03$ s. 1000 Monte-Carlo runs are performed under $\sigma = 0.01$ scenario, and the 163 runs where the ellipsoid volume of $C_{1,1}$ is smaller than $C_{1,2}$ are demonstrated. (a) the ellipsoid volume of $C_{1,1}$ and $C_{1,2}$; (b) the location error of $C_{1,1}$ and $C_{1,2}$.

In generally, the sensors have errors in their locations and an excellent localization method should be robust for the errors. For ease of illustration, we only consider the zero-mean Gaussian errors, where σ_x and σ_y are the standard deviation, and these errors are mutually independent. From Fig. 6, the location accuracy is slightly reduced as the sensor location errors increase, which indicates that the SC-MC method can tolerate the sensor location errors.

The TOA measurements interval at each sensor is related to the source emission times interval and the distance between the sources. For the large source emission times interval, the TOA measurements interval is large. When the source emission times interval is small and the distance between the sources is large, the TOA measurements interval is also large. For the combination $C_{1,1} = \{t^j_{1,l}, \cdots, t^j_{i-1,l}, t^\lambda_{i,l}, t^j_{i+1,l}, \cdots, t^j_{M,l}\}$ (proposed by (8)) where the TOA measurement $t^\lambda_{i,l}$ comes from the λth source, when the interval $\Delta t = |t^\lambda_{i,l} - t^j_{i,x}|$ (the xth, $x \neq l$ TOA measurement at the ith sensor comes from the jth source) is large, the location estimates corresponding to subsets of TOA measurements is very scattered and the ellipsoid volume is very large, which is helpful to identify the false combination. When the interval Δt is small, it is possible that the ellipsoid volume of $C_{1,1}$ is smaller than $C_{1,2} = \{t^j_{1,l}, \cdots, t^j_{i,x}, \cdots, t^j_{M,l}\}$, and the location error of $C_{1,1}$ is not significantly larger than $C_{1,2}$, as shown in Fig. 7.

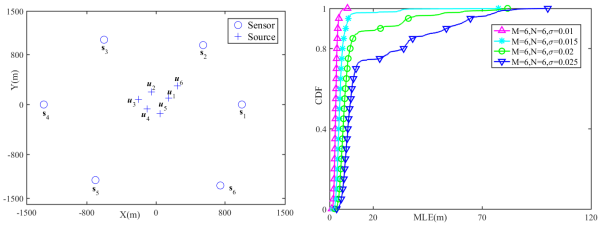

(a) (b)

FIGURE 8. Comparison of the location accuracy under different σ conditions. (a) the locations of the $M = 6$ sensors and the $N = 6$ sources; (b) the CDF of MLE for different σ.

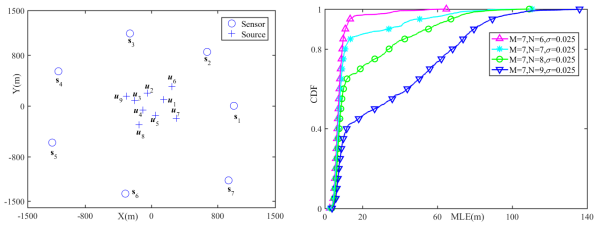

(a) (b)

FIGURE 9. Comparison of the location accuracy under different N conditions. (a) the locations of the sensors and the sources; (b) the CDF of MLE for different N.

From Fig. 7, when one sensor has two TOA measurements whose interval Δt is less than a threshold τ, the two TOA measurements can be replaced by each other and the grouping matrix with duplicated indices should also be accepted. Taking into account the location error of the hyperbolic localization algorithm itself, the interval threshold τ has a positive correlation with the noise σ, and in this paper, $0.05 \leq \tau \leq 0.15$.

Fig. 8(b) depicts that the location accuracy decreases with the increase of the noise level σ. When σ increases, the location error of the hyperbolic localization algorithm also increases and the location estimates corresponding to subsets of TOA measurements become more scattered, which results in a decrease in the sensitivity of the ellipsoid volume measuring the scatter of the location estimates and an increase in the mismatch probability.

From Fig. 9(b), the location accuracy decreases with the increase of N. When the number N of the sources increases, the number of the initial combinations of TOA measurements increases exponentially and the possibility that there exists a false combination minimizing the criterion function also increases. The SC-MC method needs to pick out the true combination of TOA measurements from more false combinations, which leads to a higher mismatch probability.

From Fig. 10(b), the location error is reduced with the increase of the number M of the sensors. More sensors mean more source location information, which are helpful to identify the false combinations of TOA measurements more effectively and improve the location accuracy.

C. EXPLOSION EXPERIMENTS

The explosion experiments were carried out in an open field of approximately 160 meters by 160 meters, and the locations

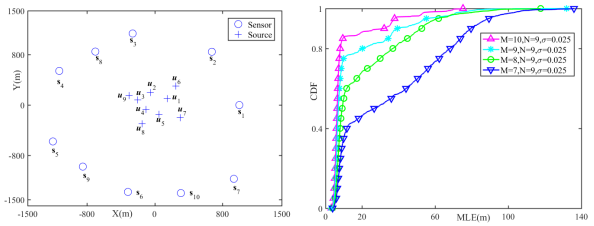

FIGURE 10. Comparison of the location accuracy under different M conditions. (a) the locations of the sensors and the sources; (b) the CDF of MLE for different M.

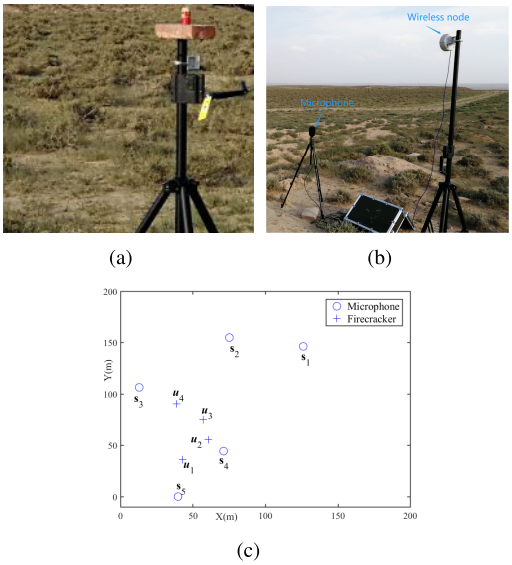

FIGURE 11. The experiment scene. (a) the firecracker; (b) the microphone and wireless node; (c) the locations of the microphones and the firecrackers.

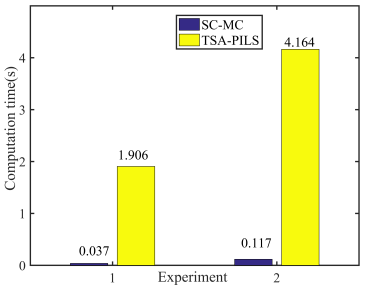

FIGURE 12. Comparison of the computation time of SC-MC and TSA-PILS.

of the $M = 5$ microphones and the $N = 4$ sources consisting of firecrackers are provided by GPS, as shown in Fig. 11(c) (the locations relative to a randomly selected reference point are shown). The wind speed can be ignored and the sound speed is $c = 343$ m/s. The time corresponding to the peak of the blast wave of the firecracker is used as the TOA measurement.

In the experiments, the CVX-TOA method is not suitable due to the small number of the microphones. Table 5 and

TABLE 5. Location error of SC-MC and TSA-PILS (m).

source	SC-MC		TSA-PILS	
	Experiment 1	Experiment 2	Experiment 1	Experiment 2
$\boldsymbol{u}_1$	1.7	1.9	2.3	2.3
$\boldsymbol{u}_2$	4.9	4.9	5.8	5.0
$\boldsymbol{u}_3$	3.1	3.3	3.6	2.7
$\boldsymbol{u}_4$	—[1]	2.2	—	3.3

[1] The firecracker did not explode.

Fig. 12 show the location error and computation time of SC-MC and TSA-PILS, respectively. It can be observed that TSA-PILS has larger location error and higher computation time than the proposed SC-MC method, which is consistent with the previous simulation results.

VI. CONCLUDING REMARKS

In this paper, a self-clustering measurement combination method is proposed for the multi-source localization problem. The method exploits the correlation between the TOA measurements at different sensors, and a three-step heuristic clustering algorithm is used to find the combination of TOA measurements from the same source and then estimate the location of the source. Simulation and experiment indicate that the method has higher location accuracy and lower computational cost compared with the existing methods. The presence of false or missing measurements will be considered in the future work.

APPENDIX A

Corollary 1: $\hat{\boldsymbol{u}}_j^e$ has a deviation compared with $\hat{\boldsymbol{u}}_j$.

Proof: For the combination $\{t_{1,l}^j, \cdots, t_{i-1,l}^j, t_{i,l}^\lambda, t_{i+1,l}^j, \cdots, t_{M,l}^j\}$, $\lambda \in [1, N]$ and $\lambda \neq j$, (2) should be

$$r_{j,i,1}^e = c(t_{i,l}^\lambda - t_{1,l}^j) = ||\boldsymbol{u}_\lambda - \mathbf{s}_i|| - ||\boldsymbol{u}_j - \mathbf{s}_1||. \tag{20}$$

Let $\Delta\boldsymbol{u}_{\lambda,j} = \boldsymbol{u}_\lambda - \boldsymbol{u}_j$, therefore, (3) can be written as

$$\begin{aligned} r_{j,i,1}^{e2} - \mathbf{s}_i^T\mathbf{s}_i + \mathbf{s}_1^T\mathbf{s}_1 + 2\mathbf{s}_i^T\Delta\boldsymbol{u}_{\lambda,j} - ||\Delta\boldsymbol{u}_{\lambda,j}||^2 \\ = -2[(\mathbf{s}_i - \mathbf{s}_1 - \Delta\boldsymbol{u}_{\lambda,j})^T, r_{j,i,1}^e]\boldsymbol{\varphi}_j. \end{aligned} \tag{21}$$

The estimate

$$\begin{aligned} \hat{\boldsymbol{\varphi}}_j = ((\Gamma_j^e + \Delta\Gamma_j)^T\Psi_j^{e^{-1}}(\Gamma_j^e + \Delta\Gamma_j))^{-1} \\ \times(\Gamma_j^e + \Delta\Gamma_j)^T\Psi_j^{e^{-1}}(\mathbf{h}_j^e + \Delta\mathbf{h}_j), \end{aligned} \tag{22}$$

where

$$\begin{aligned} (\Delta\mathbf{h}_j)(i) &= (2\mathbf{s}_i^T\Delta\boldsymbol{u}_{\lambda,j} - ||\Delta\boldsymbol{u}_{\lambda,j}||^2)/2, \\ (\Delta\Gamma_j)(i,:) &= [(\Delta\boldsymbol{u}_{\lambda,j})^T, 0]. \end{aligned} \tag{23}$$

The other elements in the column vector $\Delta\mathbf{h}_j$ and matrix $\Delta\Gamma_j$ are 0. In fact, $\Delta\boldsymbol{u}_{\lambda,j}$ is unknown and can only get the ghost estimate

$$\hat{\boldsymbol{\varphi}}_j^e = (\Gamma_j^{eT}\Psi_j^{e^{-1}}\Gamma_j^e)^{-1}\Gamma_j^{eT}\Psi_j^{e^{-1}}\mathbf{h}_j^e. \tag{24}$$

Therefore, the ghost target location estimate $\hat{\boldsymbol{u}}_j^e = \hat{\boldsymbol{\varphi}}_j^e(1:2)$ (the first two elements of $\hat{\boldsymbol{\varphi}}_j^e$ are the estimated location vector) has a deviation compared with $\hat{\boldsymbol{u}}_j = \hat{\boldsymbol{\varphi}}_j(1:2)$.

APPENDIX B

Corollary 2: The determinant $|\boldsymbol{\Sigma}_j^e|$ of the covariance matrix of $\hat{\boldsymbol{u}}_j^e$ is larger than $|\boldsymbol{\Sigma}_j|$ of $\hat{\boldsymbol{u}}_j$.

Proof: From (24), it assumes that $\hat{\boldsymbol{u}}_j^e = \hat{\boldsymbol{u}}_j + \boldsymbol{e}_{j,1}, \boldsymbol{u}_j^e = \boldsymbol{u}_j + \boldsymbol{e}_{j,2}, \boldsymbol{e}_{j,3} = \boldsymbol{e}_{j,1} - \boldsymbol{e}_{j,2}$, the covariance matrix

$$\begin{aligned}\boldsymbol{\Sigma}_j^e &= \mathbb{E}\{(\boldsymbol{u}_j^e - \hat{\boldsymbol{u}}_j^e)(\boldsymbol{u}_j^e - \hat{\boldsymbol{u}}_j^e)^T\} \\ &= \mathbb{E}\{(\boldsymbol{u}_j - \hat{\boldsymbol{u}}_j - \boldsymbol{e}_{j,1} + \boldsymbol{e}_{j,2})(\boldsymbol{u}_j - \hat{\boldsymbol{u}}_j - \boldsymbol{e}_{j,1} + \boldsymbol{e}_{j,2})^T\} \\ &= \mathbb{E}\{(\boldsymbol{u}_j - \hat{\boldsymbol{u}}_j - \boldsymbol{e}_{j,3})(\boldsymbol{u}_j - \hat{\boldsymbol{u}}_j - \boldsymbol{e}_{j,3})^T\} \\ &= \mathbb{E}\{(\boldsymbol{u}_j - \hat{\boldsymbol{u}}_j)(\boldsymbol{u}_j - \hat{\boldsymbol{u}}_j)^T\} + \boldsymbol{e}_{j,3}\boldsymbol{e}_{j,3}^T \\ &= \boldsymbol{\Sigma}_j + \boldsymbol{e}_{j,3}\boldsymbol{e}_{j,3}^T. \end{aligned} \tag{25}$$

$\boldsymbol{e}_{j,3}\boldsymbol{e}_{j,3}^T$ is a positive-definite matrix, and the determinant $|\boldsymbol{\Sigma}_j^e|$ is larger than $|\boldsymbol{\Sigma}_j|$.

REFERENCES

[1] W. Dargie and C. Poellabauer, *Fundamentals of Wireless Sensor Networks: Theory and Practice*. New York, NY, USA: Wiley, 2010.
[2] K. Sohraby, D. Minoli, and T. Znati, *Wireless Sensor Networks: Technology, Protocols, and Applications*. New York, NY, USA: Wiley, 2007.
[3] M. Brandstein and D. Ward, *Microphone Arrays*. Berlin, Germany: Springer-Verlag, 2001.
[4] A. Bertrand, "Applications and trends in wireless acoustic sensor networks: A signal processing perspective," in *Proc. 18th IEEE Symp. Commun. Veh. Technol. Benelux (SCVT)*, Nov. 2011, pp. 1–6.
[5] P.-J. Chung and J. F. Boehme, "The methodology of the maximum likelihood approach: Estimation, detection, and exploration of seismic events," *IEEE Signal Process. Mag.*, vol. 29, no. 3, pp. 40–46, May 2012.
[6] J.-M. Valin, F. Michaud, J. Rouat, and D. Letourneau, "Robust sound source localization using a microphone array on a mobile robot," in *Proc. IEEE/RSJ Int. Conf. Intell. Robots Syst.*, Oct. 2003, pp. 1228–1233.
[7] S. Wen, L. Xing, X. Q. Hu, and H. Zhang, "Measurement-converted Kalman filter tracking with Gaussian intensity attenuation signal in wireless sensor networks," *Int. J. Distrib. Sensor Netw.*, vol. 13, no. 4, pp. 1–13, Apr. 2017.
[8] H. Wang and P. Chu, "Voice source localization for automatic camera pointing system in videoconferencing," in *Proc. IEEE Int. Conf. Acoust., Speech, Signal Process.*, Apr. 1997, pp. 187–190.
[9] A. H. Sayed, A. Tarighat, and N. Khajehnouri, "Network-based wireless location: Challenges faced in developing techniques for accurate wireless location information," *IEEE Signal Process. Mag.*, vol. 22, no. 4, pp. 24–40, Jul. 2005.
[10] X. Sheng and Y.-H. Hu, "Maximum likelihood multiple-source localization using acoustic energy measurements with wireless sensor networks," *IEEE Trans. Signal Process.*, vol. 53, no. 1, pp. 44–53, Jan. 2005.
[11] D. Li and Y. H. Hu, "Energy-based collaborative source localization using acoustic microsensor array," *EURASIP J. Adv. Signal Process.*, vol. 4, pp. 321–337, Mar. 2003.
[12] E. Dranka and R. Coelho, "Robust maximum likelihood acoustic energy based source localization in correlated noisy sensing environments," *IEEE J. Sel. Topics Signal Process.*, vol. 9, no. 2, pp. 259–267, Mar. 2015.
[13] E. Masazade, R. Niu, P. K. Varshney, and M. Keskinoz, "Energy aware iterative source localization for wireless sensor networks," *IEEE Trans. Signal Process.*, vol. 58, no. 9, pp. 4824–4835, Sep. 2010.
[14] L. G. Taff, "Target localization from bearings-only observations," *IEEE Trans. Aerosp. Electron. Syst.*, vol. 33, no. 1, pp. 2–10, Jan. 1997.
[15] L. M. Kaplan, Q. Le, and N. Molnar, "Maximum likelihood methods for bearings-only target localization," in *Proc. IEEE Int. Conf. Acoust., Speech, Signal Process.*, May 2001, pp. 3001–3004.
[16] Y. Oshman and P. Davidson, "Optimization of observer trajectories for bearings-only target localization," *IEEE Trans. Aerosp. Electron. Syst.*, vol. 35, no. 3, pp. 892–902, Jul. 1999.
[17] M. Gavish and A. J. Weiss, "Performance analysis of bearing-only target location algorithms," *IEEE Trans. Aerosp. Electron. Syst.*, vol. 28, no. 3, pp. 817–828, Jul. 1992.
[18] Y. T. Chan and K. C. Ho, "A simple and efficient estimator for hyperbolic location," *IEEE Trans. Signal Process.*, vol. 42, no. 8, pp. 1905–1915, Aug. 1994.
[19] Y. Huang, J. Benesty, G. W. Elko, and R. M. Mersereati, "Real-time passive source localization: A practical linear-correction least-squares approach," *IEEE Trans. Speech Audio Process.*, vol. 9, no. 8, pp. 943–956, Nov. 2001.
[20] C. Militello and S. R. Buenafuente, "An exact noniterative linear method for locating sources based on measuring receiver arrival times," *J. Acoust. Soc. Amer.*, vol. 121, no. 6, p. 3595, Mar. 2007.
[21] M. S. Brandstein, J. E. Adcock, and H. F. Silverman, "A closed-form location estimator for use with room environment microphone arrays," *IEEE Trans. Speech Audio Process.*, vol. 5, no. 1, pp. 45–50, Jan. 1997.
[22] J. Smith and J. Abel, "Closed-form least-squares source localization estimation form range-difference measurements," *IEEE Trans. Acoust., Speech, Signal Process.*, vol. ASSP-35, no. 12, pp. 1661–1662, Dec. 1987.
[23] L. Yang and K. C. Ho, "An approximately efficient TDOA localization algorithm in closed-form for locating multiple disjoint sources with erroneous sensor positions," *IEEE Trans. Signal Process.*, vol. 57, no. 12, pp. 4598–4615, Dec. 2009.
[24] T.-K. Le and N. Ono, "Closed-form and near closed-form solutions for TOA-based joint source and sensor localization," *IEEE Trans. Signal Process.*, vol. 64, no. 18, pp. 4751–4766, Sep. 2016.
[25] T.-K. Le and N. Ono, "Robust TDOA-based joint source and microphone localization in a reverberant environment using medians of acceptable recovered TOAs," in *Proc. IEEE Int. Workshop Acoustic Signal Enhancement (IWAENC)*, Sep. 2016, pp. 1–5.
[26] T.-K. Le and N. Ono, "Closed-form and near closed-form solutions for TDOA-based joint source and sensor localization," *IEEE Trans. Signal Process.*, vol. 65, no. 5, pp. 1207–1221, Mar. 2017.
[27] M. Cobos, F. Antonacci, A. Alexandridis, A. Mouchtaris, and B. Lee, "A survey of sound source localization methods in wireless acoustic sensor networks," *Wireless Commun. Mobile Comput.*, vol. 2017, no. 15, Aug. 2017, Art. no. 3956282.
[28] J. Y. Shen and A. F. Molisch, "Estimating multiple target locations in multi-path environments," *IEEE Trans. Wireless Commun.*, vol. 13, no. 8, pp. 4547–4559, Aug. 2014.
[29] D. J. Torrieri, "Statistical theory of passive location systems," *IEEE Trans. Aerosp. Electron. Syst.*, vol. AES-20, no. 2, pp. 183–198, Mar. 1984.
[30] G. Simon, M. Maróti, A. Lédeczi, G. Balogh, B. Kusy, A. Nádas, G. Pap, J. Sallai, and K. Frampton, "Sensor network-based countersniper system," in *Proc. 2nd Int. Conf. Embedded Netw. Sensor Syst.*, Nov. 2001, pp. 1–12.
[31] S. Venkateswaran and U. Madhow, "Localizing multiple events using times of arrival: A parallelized, hierarchical approach to the association problem," *IEEE Trans. Signal Process.*, vol. 60, no. 10, pp. 5464–5477, Oct. 2012.
[32] H. Shen, Z. Ding, S. Dasgupta, and C. M. Zhao, "Multiple source localization in wireless sensor networks based on time of arrival measurement," *IEEE Trans. Signal Process.*, vol. 62, no. 8, pp. 1938–1949, Apr. 2014.
[33] S. A. Stotts, J. L. Martin, and N. R. Bedford, "Multiple-source localization using GPS technology and received arrival time structure analysis in an air-deployed system," *IEEE J. Ocean. Eng.*, vol. 22, no. 3, pp. 576–582, Jul. 1997.
[34] R. O. Duda, P. E. Hart, and D. G. Stork, *Pattern Classification*. New York, NY, USA: Wiley, 2001.
[35] K. R. Pattipati, S. Deb, Y. Bar-Shalom, and R. B. Washburn, "A relaxation algorithm for the passive sensor data association problem," in *Proc. Amer. Control Conf.*, Jun. 1989, pp. 2617–2627.
[36] S. Deb, K. R. Pattipati, and Y. Bar-Shalom, "A multisensor-multitarget data association algorithm for heterogeneous sensors," *IEEE Trans. Aerosp. Electron. Syst.*, vol. 29, no. 2, pp. 560–568, Apr. 1993.
[37] K. C. Ho, "Bias reduction for an explicit solution of source localization using TDOA," *IEEE Trans. Signal Process.*, vol. 60, no. 5, pp. 2101–2114, May 2012.

XINWEI GUO received the B.S. degree from Shaanxi Normal University, Xi'an, China, in 2016. He is currently pursuing the Ph.D. degree with the Institute of Acoustics, Chinese Academy of Sciences, Beijing. His current research interests include wireless sensor networks, acoustic signal processing, and source localization.

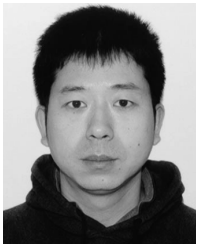

ZHIFEI CHEN received the Ph.D. degree from Northwestern Polytechnical University, Xi'an, China, in 2011. From 2016 to 2018, he held a postdoctoral position with the Institute of Acoustics, Chinese Academy of Sciences. His current research interests include wireless sensor networks and acoustic signal processing.

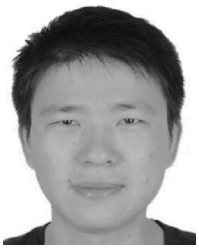

XIAOQING HU received the Ph.D. degree from the South China University of Technology, Guangzhou, China, in 2013. From 2011 to 2013, he was a Visiting Ph.D. Student with the Department of Electrical and Computer Engineering, University of Wisconsin–Madison. From 2013 to 2015, he held a postdoctoral position with the Institute of Acoustics, Chinese Academy of Sciences, where he is currently an Associate Professor. His current research interests include wireless sensor networks, Bayesian statistics, and acoustic signal processing.

XIAODONG LI received the Ph.D. degree in physical acoustics from the Institute of Acoustics, Chinese Academy of Sciences, Beijing, China, in 1995. Since 1995, he has been with the Institute of Acoustics, Chinese Academy of Sciences, where he is currently a Professor and the Director of the Communication Acoustic Laboratory. His current research interests include physical acoustics and signal processing. He is an Executive Member of the Chinese Acoustics Society.